Quick assessment of chicken spoilage based on hyperspectral NIR spectra combined with partial least squares regression

Shengqi Jiang[1], Hongju He[1,2,3*], Hanjun Ma[1,2], Fusheng Chen[3], Baocheng Xu[4], Hong Liu[5], Mingming Zhu[1], Zhuangli Kang[1], Shengming Zhao[1]

(1. *School of Food Science, Henan Institute of Science and Technology, Xinxiang 453003, Henan, China*;
2. *Henan Institute of Science and Technology, Postdoctoral Research Base, Xinxiang 453003, Henan, China*;
3. *College of Grain, Oil and Food, Henan University of Technology, Zhengzhou 450000, China*;
4. *College of Food and Bioengineering, Henan University of Science and Technology, Luoyang 471003, Henan, China*;
5. *Key Laboratory of the Ministry of Education of Tropical Medicine, Hainan Normal University, Haikou 570203, China*)

Abstract: *Pseudomonas* spp. and *Enterobacteriaceae* are dominant spoilage bacteria in chicken during cold storage (0°C-4°C). In this study, high resolution spectra in the range of 900-1700 nm were acquired and preprocessed using Savitzky-Golay convolution smoothing (SGCS), standard normal variate (SNV) and multiplicative scatter correction (MSC), respectively, and then mined using partial least squares (PLS) algorithm to relate to the total counts of *Pseudomonas* spp. and *Enterobacteriaceae* (PEC) of fresh chicken breasts to predict PEC rapidly. The results showed that with full 900-1700 nm range wavelength, MSC-PLS model built with MSC spectra performed better than PLS models with other spectra (RAW-PLS, SGCS-PLS, SNV-PLS), with correlation coefficient (R_P) of 0.954, root mean square error of prediction (RMSEP) of 0.396 $\log_{10}$ CFU/g and residual predictive deviation (RPD) of 3.33 in prediction set. Based on the 12 optimal wavelengths (902.2 nm, 905.5 nm, 923.6 nm, 938.4 nm, 946.7 nm, 1025.7 nm, 1124.4 nm, 1211.6 nm, 1269.2 nm, 1653.7 nm, 1691.8 nm and 1693.4 nm) selected from MSC spectra by successive projections algorithm (SPA), SPA-MSC-PLS model had R_P of 0.954, RMSEP of 0.397 $\log_{10}$ CFU/g and RPD of 3.32, similar to MSC-PLS model. The overall study indicated that NIR spectra combined with PLS algorithm could be used to detect the PEC of chicken flesh in a rapid and non-destructive way.

Keywords: hyperspectral NIR spectra, chicken, dominant spoilage, partial least squares regression, quick assessment
DOI: 10.25165/j.ijabe.20211401.5726

Citation: Jiang S Q, He H J, Ma H J, Chen F S, Xu B C, Liu H, et al. Quick assessment of chicken spoilage based on hyperspectral NIR spectra combined with partial least squares regression. Int J Agric & Biol Eng, 2021; 14(1): 243–250.

1 Introduction

Due to high protein, low fat and cholesterol, as well as good flesh taste, chicken is consumed in large quantities and has become one of the most popular meat products[1,2]. Raw fresh chicken flesh is preferred and consumed by human beings within several days after slaughter. However, chilled chicken is easy contaminated by microorganisms during production, transportation, sales and storage under the current conditions, because of a good environment that contains sufficient moisture, protein and other nutrients for microbial growth and reproduction, especially dominant spoilage microorganisms, which always results in the flesh spoilage and quality losses.

In our preliminary experiment, it was found that *Pseudomonas* spp. and *Enterobacteriaceae* are two dominant spoilage microorganisms in chicken at early days during cold storage (0°C-4°C), which is in accordance with other reports[3-7]. *Pseudomonas* spp. is one kind of gram-negative, rod-shaped and aerobic organism and can grow and reproduce with simple nutrients[8]. *Enterobacteriaceae* is one group of facultatively anaerobic and gram-negative rod-shaped bacteria without spores and can transform carbohydrates into acids and gas during fermentation[9]. With the contamination caused by the two kinds of bacteria, the color, smell and appearance of chicken flesh deteriorate gradually, and that could influence the consumer desire to purchase, as well as cause the potential harm for human health. The total counts of *Pseudomonas* spp. and *Enterobacteriaceae* (PEC) can be used for the spoilage evaluation of chicken flesh.

Many conventional methods are currently available to detect microbial spoilage such as the standard colony-counting method[10], polymerase chain reaction (PCR)[11] and immunology-based approaches[12,13]. The colony-counting method is a common method of counting live bacteria, which is based on the phenomenon that a colony is formed by microorganisms on solid culture medium. This method is a classical counting method with good repeatability, good parallelism, large linear range and low technical requirement. Polymerase chain reaction (PCR) is an in

Received date: 2020-02-11 **Accepted date:** 2020-11-12
Biographies: Shengqi Jiang, Master, research interest: food nondestructive analysis and detection, Email: shq_jiang@163.com; **Hanjun Ma**, PhD, Professor, research interest: meat processing and quality control, Email: xxhjma@126.com; **Fusheng Chen**, PhD, Professor, research interest: food resource development and utilization, Email: fushengc@haut.edu.cn; **Baocheng Xu**, PhD, Associate Professor, research interest: oil component control technology, Email: xbc76@163.com; **Hong Liu**, PhD, Professor, research interest: food engineering, Email: lhyd123@126.com; **Mingming Zhu**, PhD, research interest: processing and storage of agricultural products, protein purification, Email: happyzhumingming@126.com; **Zhuangli Kang**, PhD, Associate Professor, research interest: meat processing, Email: kzlnj1988@163.com; **Shengming Zhao**, PhD, research interest: food safety and control, Email: zhaoshengming2008@126.com.

***Corresponding author: Hongju He**, PhD, Professor, research interest: food nondestructive analysis and detection. Henan Institute of Science and Technology, Postdoctoral Research Base, Xinxiang 453003, Henan, China. Tel: +86-373-3040674, +86-13598726097, Fax: +86-373-3040674, Email: hongju_he007@ 126.com.

vitro DNA or RNA amplification technique with high specificity, high sensitivity and high efficiency. Immunology-based approaches are new detection method based on antigen-antibody specific immune reaction combined with fluorescence technology and chromatography technology. It has the advantages of high efficiency, no pollution and high accuracy. As is well known, these methods are useful, effective and reliable, but they are destructive, laborious and require more time. In addition, these methods are not suitable for the large-scale and on-site quick microbial evaluation of chicken products. New technologies or methods should be developed to meet the increasing requirements for rapid and nondestructive determination. Several advanced optical technologies have been studied and reported in meat quality evaluation with satisfying results, such as computer vision[14,15], near-infrared (NIR) spectroscopy[16-18] and Raman spectroscopy[19-21].

Among, NIR spectroscopy as one effective and non-contact technique has been investigated for meat quality assessment, mainly in terms of chemical and physical attributes[22-25]. Also, NIR spectroscopy has been used for the detection of chicken meat products. Alexandrakis et al.[26] was able to correctly classify spoilage samples from day 8 and day 14 by using near-infrared spectroscopy combined with principal component analysis through the degree of proteolysis but failed to completely discriminate between pre-spoilage day 0 and day 4 samples. Jia et al.[27] predicted the pH value of fresh chicken breast pieces nondestructive by using visible near-infrared spectroscopy combined with partial least squares and competitive adaptive reweighting sampling method, and the values of *R*, RMSEP and RPD measured by the independent test set were 0.73, 0.29 and 3.55, respectively. Xiong et al.[28] predicted the reference value of thiobarbituric acid in chicken with partial least squares and successive projections algorithm within the range of 400-1000 nm, and obtained acceptable results with *Rp* of 0.801 and RMSEP of 0.157 mg/100 g. There are few studies on chicken PEC. Given this, this study attempted to mine the data from high resolution spectra for the PEC evaluation. The specific objectives of this study were to:

(1) Acquire high resolution NIR spectra of chicken samples in the range of 900-1700 nm at different cold storage time using a hyperspectral imaging system;

(2) Carry out the spectral pre-processing to eliminate the interference from the instrument itself and the surrounding environment;

(3) Mine useful information from the NIR spectra using partial least squares (PLS) algorithm to relate to the reference PEC values measured by standard pour plate method;

(4) Select optimal spectral information using the successive projections algorithm (SPA) to optimize the PLS model.

2 Materials and methods

2.1 Sample preparation

Sixty fresh raw chicken breasts were supplied by Dayong Food Co., Ltd., Hebi, Henan, China and the size of all chicken breasts was measured with the length of (15±1.0) cm and width of (9±1.0) cm. All the chicken samples were vacuum-packed and transported on ice to Meat Processing & Quality Control Lab, Henan Institute of Science and Technology, Xinxiang, Henan, China. Then, each sample was cut into cubed samples (~10 g) with a size of 3 cm×3 cm×1 cm (length×width×thickness). A total of 132 samples were finally achieved, labeled and stored at 0°C-4°C for 7 d. Figure 1 is the original image of the chicken breast taken before collecting HSI images. As can be seen from Figure 1, the microbial spoilage of chicken becomes more and more serious with the increase of storage time.

Figure 1 Original image of the chicken breast at 0°C-4°C for 7 d

2.2 Spectral data extraction

In this study, the spectra of chicken samples were collected by a NIR (900-1700 nm) hyperspectral imaging system (HSI-eNIR-XC130, Isuzu Optics Corp., Taiwan) which consists of a spectrograph (ImSpector V10E, Spectral Imaging Ltd, Oulu, Finland), a CCD camera (DL-604 M, Andor, Ireland), a lens (OLE2, Schneider, German) a moving table (IRCP0076-1COMB, Isuzu Optics Corp, Taiwan, China), illumination units (Illumination Technologies Inc, New York, USA) and a computer installed with Spectral Image software and HSI Analyzer software (Isuzu Optics Corp, Taiwan) (Figure 2). The illumination unit is a halogen source. In-chip binning performed. *F*-number of the lens was set 2.0 during image acquisition. The distance from the lens to the moving table was 45 cm.

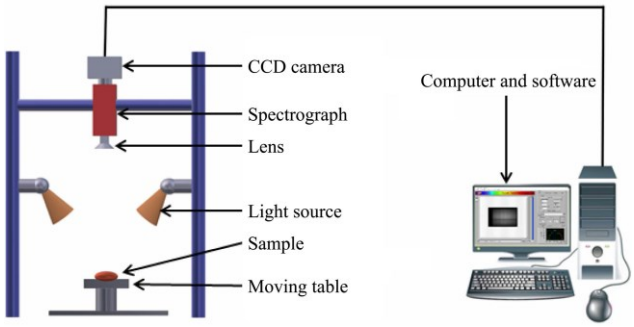

Figure 2 Schematic diagrams of main components of the hyperspectral imaging systems

Before spectral data collection, a number of samples to be tested should be taken from the refrigerator at 0°C-4°C and placed at room temperature until they return to room temperature. For the collection procedure, the samples were first put on the moving table and then scanned by the system with the moving speed of

6.33 mm/ms, the spatial resolution of 0.25 mm and the exposure time of 4.25 ms. After scanning, the hyperspectral images reflecting the light intensity were first obtained and then calibrated into reflectance images by using the following equation:

$$I = \frac{I_R - I_d}{I_w - I_d} \quad (1)$$

where, I is the calibrated hyperspectral image; I_R is the RAW hyperspectral image; I_d is the dark image collected by covering the camera lens completely (~0% reflectance); I_w is the white image collected by scanning the white calibration tile (300 mm×25 mm× 10 mm, HSI-eNIR-XC130, Isuzu Optics Corp., Taiwan) with the reflectance of about 99.9%.

HSI Analyzer is the self-contained software of the HSI-eNIR-XC130 hyperspectral imaging system for the processing of hyperspectral images and the extraction of information. Samples one by one were scanned and then the images were calibrated by HSI Analyzer. In specific, when the image separation was done, the spectra within the calibrated image were extracted and averaged by HSI Analyzer software. One mean spectrum (486 wavelengths with an interval of 1.65 nm) corresponding to one cubed sample was achieved and a total of 132 high resolution spectra were finally prepared.

2.3 Spectral data pre-processing

Before further spectral information mining, it is necessary to conduct spectral pre-processing to eliminate the interference of noise produced from the instrument itself and the surrounding environment during the spectral information acquisition. In this study, Savitzky-Golay convolution smoothing (SGCS), standard normal variate (SNV) and multiplicative scatter correction (MSC) were applied for the spectral data pre-processing by software Unscrambler 9.7 (CAMO, Oslo, Norway).

SGCS is commonly used to eliminate random noise and improve the signal-to-noise ratio[29,30]. The spectra of the samples were treated by SGCS with the number of smooths 3, the number of smoothing points of 3 and the polynomial order of 0. SNV performs well in removing the additive baseline and the multiplicative signal effects caused by light scattering and can improve the accuracy of spectral data[31,32]. MSC is mainly used for light scattering correction and aims to remove multiplicative noise caused by the physical structure of samples[27,33]. The equation for MSC is as follows:

(1) Calculate the average spectrum of all sample spectra

$$\bar{A}_j = \frac{1}{n}\sum_{i=1}^{n} A_{i,j} \quad (2)$$

(2) Linear regression was performed on the spectrum and average spectrum of each sample to obtain the regression coefficients m_i and b_i

$$A_i = m_i \bar{A} + b \quad (3)$$

(3) Calculate the corrected spectrum

$$A_{i(MSC)} = \frac{(A_i - b_i)}{m_i} \quad (4)$$

In the above equations, i=1, 2,⋯, n, n is the number of samples; j is the number of waves; $\bar{A}$ is the average spectrum of sample spectra, nm; A is the spectrum of a sample, nm; m and b are the regression coefficients of linear regression.

2.4 Microbial determination

After the image acquisition, the microbial determination was carried out using the standard plate colony counting method. In specific, each sample was immediately put into a sterile blender bag (Stomacher, London, UK) and homogenized with 90 mL buffered peptone water (0.1% peptone+0.85% NaCl). Decimal dilutions were then obtained by adding 1 mL bacteria suspension into 9 mL buffered peptone water. Subsequently, 0.1 mL bacteria suspension was quickly taken and added into plate count agar, and then spread bacteria solution evenly with sterile inoculation rods. *Pseudomonas* was incubated by CFC-selective agar (CM559+SR103, Oxoid, Basingstoke, UK) at 25°C for 48 h and *Enterobacteriaceae* was incubated by Violet Red Bile Glucose Agar (VRBGA, CM0485, Oxoid, Basingstoke, UK) at 37°C for 24 h. After cultivation, the microbial colony count between 30 and 300 was recorded and transformed into common ten-based logarithm values ($\log_{10}$ CFU/g). The PEC was the total of *Pseudomonas* counts and *Enterobacteriaceae* counts. The PEC population changes during storage at 0°C-4°C for 7 d are shown in Figure 3.

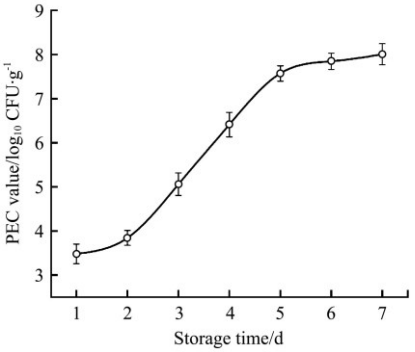

Figure 3 Population changes of PEC during storage at 0°C-4°C for 7 d

2.5 Model establishment and assessment

Partial least squares (PLS) algorithm is commonly useful and effective in spectral data mining when the number of wavelengths is larger than the number of samples and meanwhile there is high collinearity among the wavelengths[34]. In this study, PLS was adopted to mine the extracted NIR spectra (900-1700 nm) to establish the quantitative relationship between spectral data and the reference PEC values.

The performance of PLS models was assessed and compared by correlation coefficient (R) and root mean square error (RMSE) in calibration set (R_C and RMSEC) and prediction set (R_P and RMSEP), respectively. In general, a good PLS model always has high R values (R_C and R_P) and low RMSE values (RMSEC & RMSEP). Robustness and residual predictive deviation (RPD) can also be used to evaluate the performance of the model. Robustness is indicated by the value of the $|\text{RMSEC}-\text{RMSEP}|$[35]. A low absolute difference between RMSEC and RMSEP also indicates good robustness of PLS model. RPD is the ratio of the standard deviation of the prediction set to the RMSE[36]. When the value of RPD is between 1.75 and 2.25, the performance of the model is moderately useful. When the value of RPD is between 2.25 and 3.00, the performance of the model is moderately successful. When the value of RPD is between 3.00 and 4.00, the performance of the model is successful. When the value of RPD is greater than 4.00, the performance of the model is excellent.

2.6 Optimal wavelength selection and model optimization

The hundreds of spectra extracted from hyperspectral images often contain large amounts of redundant information and similar spectral information among contiguous wavelengths, which are not helpful in data processing and model performance[37]. Therefore, it is necessary to conduct wavelength selection to retain the most

useful spectral information and remove the useless information from the full wavelength range, which will accelerate the data calculation speed and also improve the model prediction accuracy[38,39].

Continuous projection algorithm (SPA) is a forward cyclic variable selection method, which starts with one variable, each cycle, and calculates the size of the projection of this variable on other unselected variables, and introduces the variable with the largest projection vector into the wavelength combination until the cycle is N times. When the number of wavelengths and the RMSE is minimized, the variable combination with the least redundant information is selected to solve problems such as information overlap and collinearity[40,41]. By using this method, the optimal wavelengths in the 900-1700 nm range were selected via software Matlab R2010a (The Mathworks, Inc., Natick, MA, USA), and the PLS models established with full 486 wavelengths were optimized with the selected optimal wavelengths to predict PEC in chicken. The performance of the optimized PLS models was also evaluated and compared in terms of *R* and RMSE values.

3 Results and discussion

3.1 Reference PEC values

The reference PEC values of the 132 cubed samples were obtained and shown in Table 1. All the values were then sorted from smallest to largest, and one in four was taken into the prediction set and the remains were put into the calibration set[42]. As a result, 99 samples were used for calibration and the rest of 33 samples were used for prediction, which can be seen in Table 1. As shown in Table 1, the maximum value of the correction set and the prediction set are 8.681 $\log_{10}$ CFU/g and 8.041 $\log_{10}$ CFU/g, the minimum value of the correction set and the prediction set are 3.079 $\log_{10}$ CFU/g and 3.146 $\log_{10}$ CFU/g, and the standard deviation of the correction set and the prediction set are 0.134 $\log_{10}$ CFU/g and 0.226 $\log_{10}$ CFU/g, respectively.

Table 1 Reference PEC values ($\log_{10}$ CFU/g) measured by the standard pour plate method

Sample set	Number of samples	Maximum	Minimum	Mean	SD
Calibration set	99	8.681	3.079	5.412	0.134
Prediction set	33	8.041	3.146	5.370	0.226

Note: SD: Standard deviation.

3.2 Spectral features of chicken samples

All the extracted average spectra of cubed chicken samples in the region of 900-1700 nm are shown in Figure 4. The changing trends of spectra were similar before and after pre-processing. As can be seen, for the four plots, there are two obvious absorption peaks at around 980 nm and 1200 nm which are attributed to O-H stretching second overtone and C-H stretching second overtone, respectively[26,43]. However, typical protein absorption information was not found as it was masked by water information, resulting from the over 70% of the water in chicken flesh. Although no absorption peak was found regarding PEC, appropriate chemometric algorithms could be used to mine the spectra from the full range to relate to PEC.

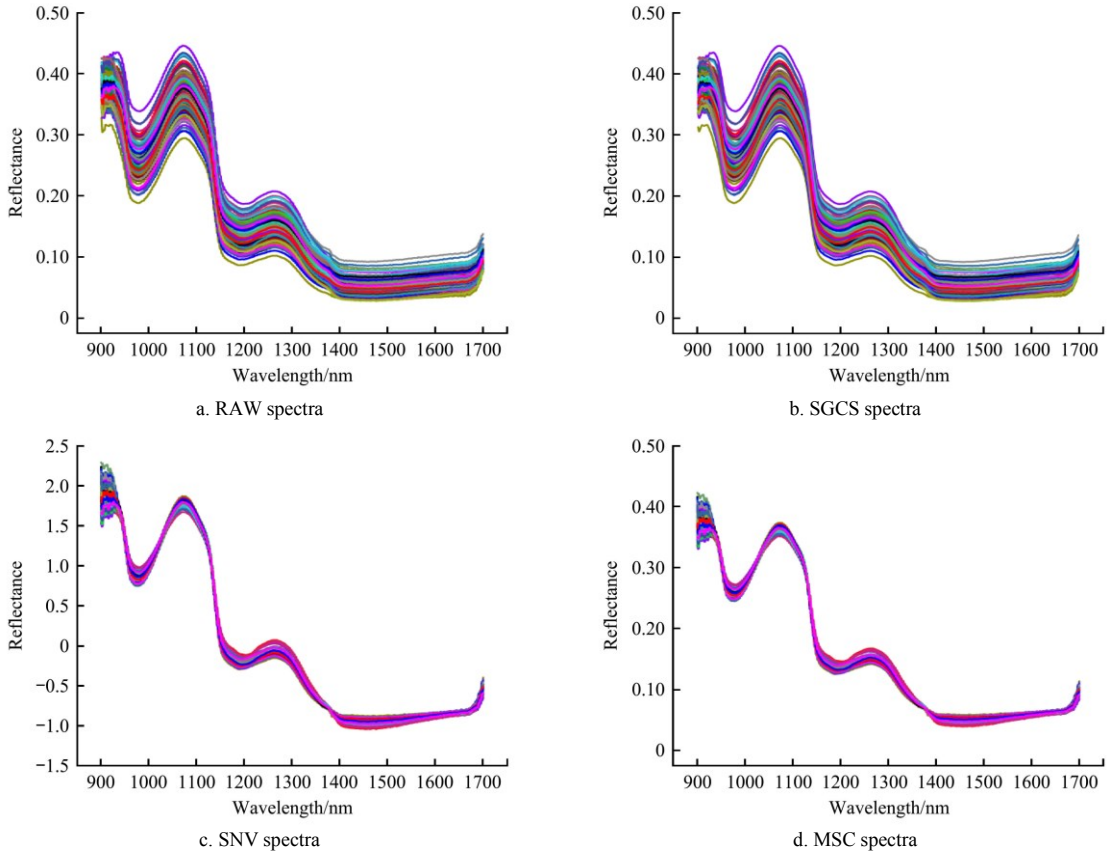

Figure 4 Average spectra characteristics of chicken samples in the region of 900-1700 nm

3.3 PLS model for predicting PEC values using full wavelength

To find the quantitative relationship between spectra and reference PEC values, PLS algorithm was implemented by inputting a matrix with 132 samples×486 wavelengths. Where, the sub-matrix of 99 samples×486 wavelengths was used for calibration and the rest sub-matrix of 33 samples×486 wavelengths was for prediction. With RAW, SGCS, SNV and MSC spectra, four full wavelengths PLS models were established and their performances were evaluated and shown in Table 2. It can be seen that the *R* values (R_C and R_P) of all the four PLS models are

~0.950, which indicates a good linear correlation between spectra and PEC values. The similar values of |RMSEC-RMSEP| also showed similar performance of the four PLS models in predicting PEC values. Besides, the RPD values were larger than 3, indicating that the four models were moderately successful. In a word, the high R and RPD values and the small |RMSEC-RMSEP| values indicated the good ability of the PLS models in predicting PEC values of chicken breasts.

Table 2 PLS models for predicting PEC by using the full range spectra

Spectra	Model	Number of wavelengths	Calibration set		Prediction set		$\lvert R_C-R_P\rvert$	|RMSEC-RMSEP|	RMSEP/RMSEC	RPD
			R_C	RMSEC	R_P	RMSEP				
RAW	RAW-PLS	486	0.967	0.340	0.949	0.415	0.018	0.075	1.220	3.18
SGCS	SGCS-PLS	486	0.970	0.324	0.952	0.405	0.018	0.081	1.250	3.26
SNV	SNV-PLS	486	0.967	0.339	0.954	0.396	0.013	0.057	1.168	3.33
MSC	MSC-PLS	486	0.967	0.339	0.954	0.397	0.013	0.058	1.171	3.32

3.4 Optimal wavelengths selected by SPA

The optimal wavelengths from the RAW, SGCS, SNV and MSC spectra were respectively selected by using SPA method among the full 900-1700 nm range. The results are shown in Figures 5-8. Figure 5a, Figure 6a, Figure 7a and Figure 8a show the RMSE values with the increase of the number of optimal wavelengths selected from the RAW, SGCS, SNV and MSC spectra, respectively. And Figure 5b, Figure 6b, Figure 7b and Figure 8b show the specific positions of the optimal wavelengths selected from the RAW, SGCS, SNV and MSC spectra, respectively. Different pretreatment spectra have different optimal wavelength screening results. The optimal wavelength number of four pretreatment spectra screened by SPA method is between 12 and 13, and the wavelength reduction is between 97% and 98%. The minimum number of optimal wavelengths was 12 for SGCS and MSC spectra and 13 for Raw and SNV spectra. These optimal wavelengths were considered as the most useful wavelengths for the prediction of PEC in chicken.

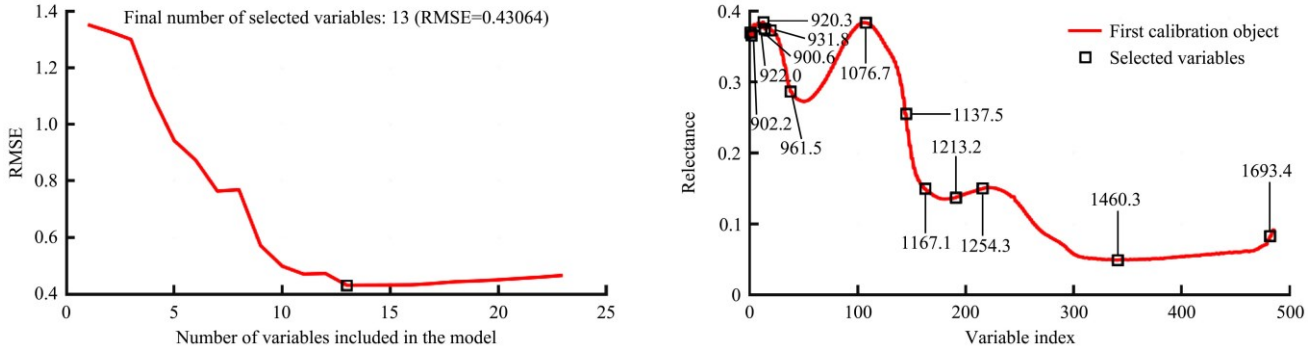

a. Number of variables included in the model b. Optimal wavelength location

Figure 5 Selection of optimal wavelengths from RAW spectra

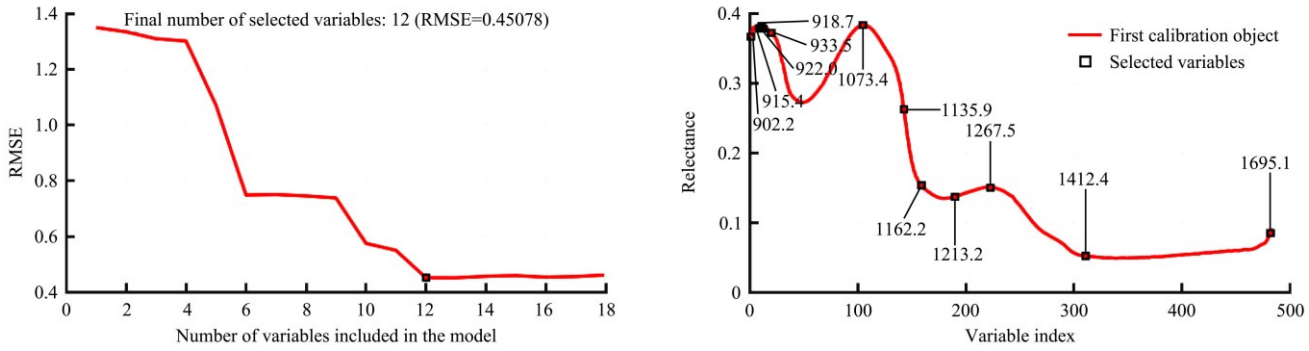

a. Number of variables included in the model b. Optimal wavelength location

Figure 6 Selection of optimal wavelengths from SGCS spectra

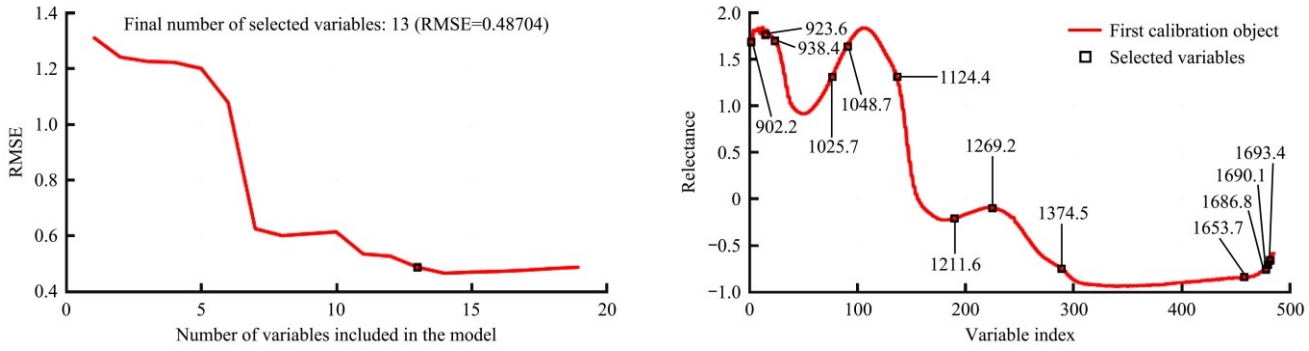

a. Number of variables included in the model b. Optimal wavelength location

Figure 7 Selection of optimal wavelengths from SNV spectra

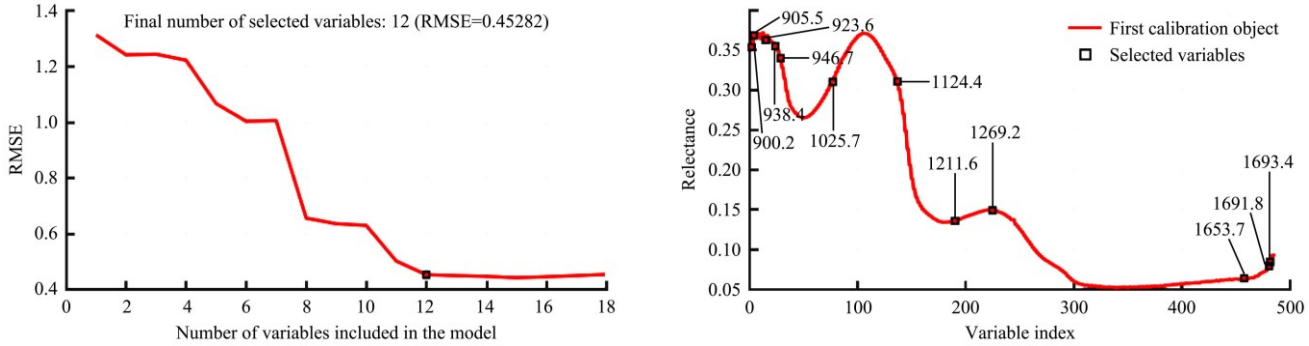

a. Number of variables included in the model b. Optimal wavelength location

Figure 8 Selection of optimal wavelengths from MSC spectra

3.5 PLS model for predicting PEC values using optimal wavelengths

Based on the above selected optimal wavelengths, four optimized PLS models were respectively established. Their performances in predicting PEC of chicken are shown in Table 3. As can be seen, all four PLS models show good accuracy and robustness in PEC prediction. Besides, the four optimized PLS models (RAW-PLS, SGCS-PLS, SNV-PLS, MSC-PLS) showed similar good performance in predicting PEC with full wavelength PLS models (SPA-RAW-PLS, SPA-SGCS-PLS, SPA-SNV-PLS, SPA-MSC-PLS), although the wavelength number reduced by 97% (486 vs. 13), 98% (486 vs. 12), 97% (486 vs. 13) and 98% (486 vs. 12), for RAW, SGCS, SNV and MSC spectra, respectively.

Table 3 PLS models for predicting PEC by using the optimal wavelengths

Spectra	Model	Number of wavelengths	Calibration set		Prediction set		$\|R_C-R_P\|$	|RMSEC−RMSEP|	RMSEP/RMSEC	RPD
			R_C	RMSEC	R_P	RMSEP				
RAW	SPA-RAW-PLS	13	0.956	0.393	0.911	0.586	0.045	0.193	1.491	2.25
SGCS	SPA-SGCS-PLS	12	0.955	0.395	0.942	0.450	0.013	0.055	1.139	2.93
SNV	SPA-SNV-PLS	13	0.945	0.438	0.923	0.515	0.022	0.077	1.176	2.56
MSC	SPA-MSC-PLS	12	0.943	0.443	0.954	0.397	0.011	0.046	0.896	3.32

Among the four optimized PLS models, the SPA-MSC-PLS model using 12 optimal wavelengths selected from MSC spectra showed the best performance in PEC prediction, with the lowest value of $|R_C-R_P|$ and |RMSEC−RMSEP| and the largest value of RPD. The *F*-test on the optimal result of PEC values was conducted for the sake of statistical soundness. As shown in Table 4, the SPA-MSC-PLS model test result of F is 1.05>1 which indicated the test on the right side, F<"F (one-tailed critical value)=1.80", p ($F\leq f$)=0.45>0.05. There was no significant difference in precision between the two groups of data of the optimal models (reference value and predicted value). As shown in Figure 9, forty contaminated chickens have been added to verify the established SPA-MSC-PLS prediction model, and the effect is expected. With the 12 wavelengths (902.2 nm, 905.5 nm, 923.6 nm, 938.4 nm, 946.7 nm, 1025.7 nm, 1124.4 nm, 1211.6 nm, 1269.2 nm, 1653.7 nm, 1691.8 nm and 1693.4 nm), the PEC value can be predicted by the following equation:

Table 4 F-test two-sample analysis of variance of optimization models

Optimization model	Item	Reference value	Predicted value
SPA-MSC-PLS	average	5.37	5.31
	variance	1.74	1.66
	Observed value	33.00	33.00
	df	32.00	32.00
	F	1.05	
	$p(F\leq f)$	0.45	
	F (one-tailed critical value)	1.80	

Note: df: Degree of freedom.

$$Y_{PEC}=-592.754-88.072X_{902.2\ nm}+74.959X_{905.5\ nm}+219.759X_{923.6\ nm}+88.072X_{902.2\ nm}+74.959X_{905.5\ nm}+219.759X_{923.6\ nm}+429.784X_{938.4\ nm}+108.801X_{946.7\ nm}+137.847X_{1025.7\ nm}+517.332X_{1124.4\ nm}+145.291X_{1211.6\ nm}+538.748X_{1269.2\ nm}+208.535X_{1653.7\ nm}-79.704X_{1691.8\ nm}+237.869X_{1693.4\ nm} \quad (5)$$

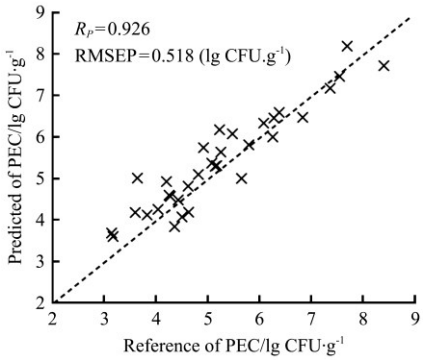

Figure 9 Test results of 40 contaminated chicken samples

4 Conclusions

Evaluation of bacterial spoilage plays an important role in guaranteeing chicken quality and safety. In this work, the potential of high resolution NIR spectra in the wavelength range of 900-1700 nm was investigated for the rapid prediction of PEC in chicken breast. By applying PLS algorithm to respectively mine the RAW, SGCS, SNV and MSC spectra. Four full wavelength PLS models were established to interpret the linear relationship between spectra and PEC values, leading to good performance with high Rs and low RMSEs. Based on the optimal wavelengths selected by SPA from the RAW, SGCS, SNV and MSC spectra, four optimized PLS models were also respectively established and

similar prediction accuracy was obtained. By comparison, SPA-MSC-PLS model built with 12 optimal wavelengths selected from MSC spectra showed the best performance with R_P of 0.954, RMSEP of 0.397 $\log_{10}$ CFU/g and RPD of 3.32. The whole results indicated the great potential of NIR for the prediction of PEC in chicken breast in a rapid and non-destructive way.

Acknowledgements

The authors acknowledged that this work was financially supported by Major Scientific and Technological Project of Henan Province (Grant No. 161100110600), Key Scientific and Technological Project of Henan Province (No. 212102310491, No. 182102310060), China Postdoctoral Science Foundation (No. 2018M632767), Henan Postdoctoral Science Foundation (No. 001801021), Youth Talents Support Project of Henan Province (No. 2018HYTP008) and Bainong Outstanding Talents Project of Henan Institute of Science and Technology (No. BNYC2018-2-27).

[References]

[1] Soncu E D. Protein oxidation and subsequent changes in chicken breast and thigh meats during long-term frozen storage. Agricultural and Food Science, 2020; 29(5): 505–514.

[2] Fu X, Chen J. A review of hyperspectral imaging for chicken meat safety and quality evaluation: application, hardware, and software. Comprehensive Reviews in Food Science and Food Safety, 2019; 18(2): 535–547.

[3] Saenz-García C E, Castañeda-Serrano P, Mercado Silva E M, Alvarado C Z, Nava G M. Insights into the identification of the specific spoilage organisms in chicken meat. Foods, 2020; 9(2): 225. doi: 10.3390/foods902025.

[4] Xu Y, Kutsanedzie F Y H, Sun H, Wang M X, Chen Q S, Guo Z M, et al. Rapid *Pseudomonas* species identification from chicken by integrating colorimetric sensors with near-infrared spectroscopy. Food Analytical Methods, 2018; 11(4): 1199–1208.

[5] Rouger A, Moriceau N, Prévost H, Remenant B, Zagorec M. Diversity of bacterial communities in French chicken cuts stored under modified atmosphere packaging. Food Microbiology, 2018; 70: 7–16.

[6] Katiyo W, Kock H L D, Coorey R, Buys E M. Sensory implications of chicken meat spoilage in relation to microbial and physicochemical characteristics during refrigerated storage. LWT-Food Science and Technology, 2020; 128: 109468. doi: 10.1016/j.lwt.2020.109468.

[7] Herbert U, Albrecht A, Kreyenschmidt J. Definition of predictor variables for MAP poultry filets stored under different temperature conditions. Poult Science, 2015; 94(3): 424–432.

[8] Sterniša M, Klančnik A, Smole Možina S. Spoilage *Pseudomonas* biofilm with Escherichia coli protection in fish meat at 5°C. Journal of the Science of Food and Agriculture, 2019; 99(10): 4635–4641.

[9] Díaz-Jiménez D, García-Meniño I, Fernández J, García V, Mora A. Chicken and turkey meat: Consumer exposure to multidrug-resistant Enterobacteriaceae including *mcr*-carriers, uropathogenic *E. coli* and high-risk lineages such as ST131. International Journal of Food Microbiology, 2020; 331: 108750. doi: 10.1016/j.ijfoodmicro.2020.108750.

[10] Shi J Y, Zhang F, Wu S B, Guo Z M, Huang X W, Hu X T, et al. Noise-free microbial colony counting method based on hyperspectral features of agar plates. Food Chemistry, 2019; 274: 925–932.

[11] Luo F F, Li Z, Dai G, Lu Y Q, He P G, Wang Q J. Simultaneous detection of different bacteria by microchip electrophoresis combined with universal primer-duplex polymerase chain reaction. Journal of Chromatography A, 2020; 1615: 460734. doi: 10.1016/j.chroma.2019.460734.

[12] Ripolles-Avila C, Martínez-Garcia M, Capellas M, Yuste J. From hazard analysis to risk control using rapid methods in microbiology: A practical approach for the food industry. Comprehensive Reviews in Food Science and Food Safety, 2020; 19(4): 1877–1907.

[13] Wang Z L, Cai R, Gao Z P, Yuan Y H. Immunomagnetic separation: An effective pretreatment technology for isolation and enrichment in food microorganisms detection. Comprehensive Reviews in Food Science and Food Safety, 2020; 19(6): 3802–3824.

[14] Kakani V, Nguyen V H, Kumar B P, Kim H, Pasupuleti V R. A critical review on computer vision and artificial intelligence in food industry. Journal of Agriculture and Food Research, 2020; 2: 100033. doi: 10.1016/j.jafr.2020.100033.

[15] Fedorov F S, Yaqin A, Krasnikov D V, Kondrashov V A, Ovchinnikov G, Kostyukevich Y, et al. Detecting cooking state of grilled chicken by electronic nose and computer vision techniques. Food Chemistry, 2020; 345: 128747. doi: 10.1016/j.foodchem.2020.128747.

[16] Zhang H L, Zhang S, Chen Y, Luo W, Huang Y F, Tao D, et al. Non-destructive determination of fat and moisture contents in Salmon (*Salmo salar*) fillets using near-infrared hyperspectral imaging coupled with spectral and textural features. Journal of Food Composition and Analysis, 2020; 92: 103567. doi: 10.1016/j.jfca.2020.103567.

[17] Anjos O, Caldeira I, Roque R, Pedro S I, Lourenço S, Canas S. Screening of Different ageing technologies of wine spirit by application of near-infrared (NIR) spectroscopy and volatile quantification. Processes, 2020; 8(6): 736. doi: 10.3390/pr8060736.

[18] Jiang H, Liu T, Chen Q S. Quantitative detection of fatty acid value during storage of wheat flour based on a portable near-infrared (NIR) spectroscopy system. Infrared Physics & Technology, 2020; 109: 103423. doi: 10.1016/j.infrared.2020.103423.

[19] Neng J, Zhang Q, Sun P L. Application of surface-enhanced Raman spectroscopy in fast detection of toxic and harmful substances in food. Biosensors and Bioelectronics, 2020: 112480. doi: 10.1016/j.bios.2020.112480.

[20] Xu Y, Zhong P, Jiang A M, Shen X, Li X M, Xu Z L, et al. Raman spectroscopy coupled with chemometrics for food authentication: A review. TrAC Trends in Analytical Chemistry, 2020: 116017. doi: 10.1016/j.trac.2020.116017.

[21] de Lima T K, Musso M, Menezes D B. Using Raman spectroscopy and an exponential equation approach to detect adulteration of olive oil with rapeseed and corn oil. Food Chemistry, 2020; 333: 127454. doi: 10.1016/j.foodchem.2020.127454.

[22] López-Maestresalas A, Insausti K, Jarén C, Pérez-Roncal C, Urrutia O, Beriain M J, et al. Detection of minced lamb and beef fraud using NIR spectroscopy. Food Control, 2019; 98: 465–473.

[23] Barbin D F, Badaró A T, Honorato D C B, Ida E Y, Shimokomaki M. Identification of turkey meat and processed products using near infrared spectroscopy. Food Control, 2020; 107: 106816. doi: 10.1016/j.foodcont.2019.106816.

[24] Peyvasteh M, Popov A, Bykov A V, Meglinski I. Meat freshness revealed by visible to near-infrared spectroscopy and principal component analysis. Journal of Physics Communications, 2020; 4(9): 095011. doi: 10.1088/2399-6528/abb322.

[25] Furtado E J G, Bridi A M, Barbin D F, Barata C C P, Peres L M, da Costa Barbon A P A, et al. Prediction of pH and color in pork meat using VIS-NIR near-infrared spectroscopy (NIRS). Food Science and Technology, 2019; 39(2): 88–92.

[26] Alexandrakis D, Downey G, Scannell A G M. Rapid non-destructive detection of spoilage of intact chicken breast muscle using near-infrared and Fourier Transform mid-infrared spectroscopy and multivariate statistics. Food and Bioprocess Technology, 2012; 5: 338–347.

[27] Jia B, Yoon S C, Zhuang H, Wang W, Li C. Prediction of pH of fresh chicken breast fillets by VNIR hyperspectral imaging. Journal of Food Engineering, 2017; 208: 57–65.

[28] Xiong Z, Sun D W, Pu H, Xie A, Han Z, Luo M. Non-destructive prediction of thiobarbituric acid reactive substances (TBARS) value for freshness evaluation of chicken meat using hyperspectral imaging. Food Chemistry, 2015; 179: 175–181.

[29] Massaoudi M, Refaat S S, Abu-Rub H, Chihi I, Oueslati F S. PLS-CNN-BiLSTM: An end-to-end algorithm-based Savitzky-Golay smoothing and evolution strategy for load forecasting. Energies, 2020; 13(20): 5464. doi: 10.3390/en13205464.

[30] Xia Z Z, Yang J, Wang J, Wang S P, Liu Y. Optimizing rice near-infrared models using fractional order Savitzky–Golay derivation (FOSGD) combined with competitive adaptive reweighted sampling (CARS). Applied Spectroscopy, 2020; 74(4): 417–426.

[31] Mishra P, Nordon A, Roger J M. Improved prediction of tablet properties with near-infrared spectroscopy by a fusion of scatter correction techniques. Journal of Pharmaceutical and Biomedical Analysis, 2020; 192: 113684. doi: 10.1016/j.jpba.2020.113684.

[32] Mishra P, Polder G, Gowen A, Rutledge D N, Roger J M. Utilising variable sorting for normalisation to correct illumination effects in close-range spectral images of potato plants. Biosystems Engineering,

2020; 197: 318–323.

[33] Wu Y, Peng S, Xie Q, Han Q J, Zhang G W, Sun H G. An improved weighted multiplicative scatter correction algorithm with the use of variable selection: Application to near-infrared spectra. Chemometrics and Intelligent Laboratory Systems, 2019; 185: 114–121.

[34] El Jabri M, Sanchez M P, Trossat P, Laithier C, Wolf V, Grosperrin P, et al. Comparison of Bayesian and partial least squares regression methods for mid-infrared prediction of cheese-making properties in Montbéliarde cows. Journal of Dairy Science, 2019; 102(8): 6943–6958.

[35] He H J, Wu D, Sun D W. Nondestructive spectroscopic and imaging techniques for quality evaluation and assessment of fish and fish products. Critical Reviews in Food Science and Nutrition, 2015; 55(6): 864–886.

[36] Malley D F, Mcclure C, Martin P D, Buckley K, Mccaughey W P. Compositional analysis of cattle manure during composting using a field-portable near-infrared spectrometer. Communications in Soil Science and Plant Analysis, 2015; 36(4-6): 455–475.

[37] Yun Y H, Li H D, Deng B C, Cao D S. An overview of variable selection methods in multivariate analysis of near-infrared spectra. TrAC Trends in Analytical Chemistry, 2019; 113: 102–115.

[38] Li J B, Wang Q Y, Xu L, Tian X, Xia Y, Fan S X. Comparison and optimization of models for determination of sugar content in pear by portable Vis-NIR spectroscopy coupled with wavelength selection algorithm. Food Analytical Methods, 2019; 12(1): 12–22.

[39] Liu D, Sun D W, Qu J, Zeng X A, Pu H, Ma J. Feasibility of using hyperspectral imaging to predict moisture content of porcine meat during salting process. Food Chemistry, 2014; 152: 197–204.

[40] Ye S, Wang D, Min S. Successive projections algorithm combined with uninformative variable elimination for spectral variable selection. Chemometrics and Intelligent Laboratory Systems, 2008; 91(2): 194–199.

[41] Moreira E D T, Pontes M J C, Galvão, R K H, Araújo M C U. Near infrared reflectance spectrometry classification of cigarettes using the successive projections algorithm for variable selection. Talanta, 2009; 79(5): 1260–1264.

[42] Wang H, He H, Ma H, Chen F, Zhu R. LW-NIR hyperspectral imaging for rapid prediction of TVC in chicken flesh. Int J Agric & Biol Eng, 2019; 12(3): 180–186.

[43] Karlsdottir M G, Arason S, Kristinsson H G, Sveinsdottir K. The application of near infrared spectroscopy to study lipid characteristics and deterioration of frozen lean fish muscles. Food Chemistry, 2014; 159(159): 420–427.